Microsyst Technol (2013) 19:1425–1431
DOI 10.1007/s00542-013-1829-5

TECHNICAL PAPER

A new hybrid fabrication process for a high sensitivity MEMS microphone

Paul C.-P. Chao · Chun-Yin Tsai · Chi-Wei Chiu · Che-Hung Tsai · Tse-Yi Tu

Received: 31 October 2012 / Accepted: 21 May 2013 / Published online: 13 June 2013

Abstract A novel multi-layer stacking capacitive type microphone is designed in this study based on theoretical analysis and numerical simulations, while fabricated via two standard stable silicon-based MEMS processes—PolyMUMPs and SOIMUMPs. The adoption of two standardized processes helps greatly to increase yield rate. The sensitivity of the microphone is first determined by an analytical model based on an equivalent circuit, which is followed by finite element (FEM) analyses on the capacitance value, static pull-in voltage and dynamic characteristics. Based on the developed analytical model, varied dimensions of the microphone are optimized and then the performance is validated by analytical simulations. In the next step, micro-fabrication of the microphone is accomplished using two standard processes, PolyMUMPs and SOIMUMPs provided by MEMSCAP. Experiments are conducted to acquire the information of pull-in voltage for safe operation and frequency response in sensitivity for performance evaluation. In the static case, experimental results show a good agreement with the analytical results with 90 Mpa residual stress assumed. As for dynamic validation, the frequency response is measured in an anechoic room adopting the exciting frequency as the audible range from 100–10 kHz. The measured sensitivity is as around 0.78 and 1.7 mV/Pa from 100 to 10 kHz, under the biases of 2 and 4.5 V, respectively. Within the audible frequency range, the proposed device maintains the loss as less as 2.7 dB (ref. to V/Pa), under 3 dB—the commonly acceptable drop within audible frequency range.

P. C.-P. Chao (✉) · C.-W. Chiu · C.-H. Tsai · T.-Y. Tu
Department of Electrical Engineering,
National Chiao Tung University,
Hsinchu 300, Taiwan
e-mail: pchao@mail.nctu.edu.tw

P. C.-P. Chao
Department of Imaging and Biophotonics,
National Chiao Tung University,
Tainan 711, Taiwan

C.-Y. Tsai
Department of Mechanical Engineering,
National Chiao Tung University,
Hsinchu 300, Taiwan

1 Introduction

One of the most successfully-developed and widely-used MEMS devices is the electrostatic condenser microphone. The main benefit of this device is its characteristic high sensitivity and small power consumption. Recent improvements in MEMS processing have resulted in the batch fabrication of low cost, high performance, miniaturized condenser microphones (Bergqvist and Rudolf 1990; Scheeper et al. 1992, 1994; Royer et al. 1983; Leinenbach et al. 2010; Chen et al. 2010; Chan et al. 2011). In addition to fabrication, past studies have accomplished static (Chao et al. 2006) and dynamic (Chao et al. 2008) pull-in analysis based on certain MEMS device geometries. In these applications, this device offers specific advantages, such as miniaturization, over traditional ECMs (electret condenser microphone). These past studies are however all fabricated in the laboratory environment which may lead to uncertainties in the future mass production (Pedersen et al. 1998; Hsu et al. 1998).

The current study therefore proposes a reliable hybrid fabrication process, which combines two standard and stable processes, PolyMUMPs (Koester et al. 2003) and SOIMUMPs (Koester et al. 2003), developed from the MEMSCAP company, aiming for designing a high

sensitivity condenser microphone. The individual processes, PolyMUMPs and SOIMUMPs, have already shown their stabilities for maintaining fabrication quality. This work then aims to adopt the two standard procedures sequentially into microphone structure design with few modified steps and specifications in the fabrication processes. The standardized process helps greatly to increase yield rate, which is still the major issue to deal with nowadays for MEMS microphone fabrication. Based on specifications, the analysis for predicting microphone sensitivity is first conducted for designing preliminary sizes of the microphone. Previous studies show that the modeling using finite element method (FEM) is efficient for fast verification about the design (Bergqvist 1993; Wang et al. 2004; Senturia 2000). Hence, the FEM analysis using commercial software, COMSOL and ANSYS, are also conducted to predict the deflection of membrane with realistic boundary conditions assumed, which are clampings at edges of the membrane. It is found that the both simulation results are close to each other and accurately predict the deflection of the vibrating membrane of the MEMS microphone.

With simulation and design completed, the MEMS microphone was then fabricated using the combined processes of PolyMUMPs and SOIMUMPs based on the proposed design concepts and compatible fabrication steps. The static characteristic, frequency response and maximum vibration amplitude of the fabricated MEMS microphone were measured. With the devices being fabricated, two approaches are adopted in experimental validation—one under static input voltage while another subjected to vibratory sound in wide frequency range. In the case with static input voltage applied to the membrane, the largest displacement of 1 μm over the entire membrane is measured by a laser Doppler vibrometer; furthermore, the pull-in phenomenon is present with acquisition of corresponding pull-in voltage and membrane deflection. In the second case with vibratory sound as the excitation, the frequency responses are measured with moderate levels of noise present. The measured sensitivity of the fabricated microphone which is under the biases of 2 and 4.5 V is around 0.78 and 1.7 mV/Pa from 100 to 10 kHz. Within this measured frequency range, the proposed device maintains the loss as less as 2.7 dB (ref. to V/Pa), under 3 dB–the commonly acceptable drop within audible frequency range.

This study is organized as follows. Section 2 presents the designed microphone structure. Section 3 performed finite element analysis and then predict pull-in and frequency response of the proposed MEMS microphone device. Section 4 states the designed fabrication process for the microphone, Sect. 5 presents experimental results. Finally, Sect. 6 concludes this study.

2 Design of the MEMS microphone

The designed microphone structure is presented in Fig. 1a. It is composed of a diaphragm as vibrating membrane and a metal backplate as the electrode. The diaphragm is pressure sensitive and deforms as a flexible plate in a parallel-plate capacitor. Figure 1b shows the layout mask of the proposed MEMS device. Through a systematically simulation analysis, the basic sensitivity formula (Bergqvist and Rudolf 1990) shows that the sensitivity of the basic square microphone is in a direct proportion with DC bias voltage, while in an inverse proportion with the air gap. The basic design goal herein is to increase the sensitivity of the microphones.

The mechanical behavior of the microphone can be regarded as the part of an equivalent circuit, which relates forces (potential) and velocities (flow) in the microphone structure, aiming to predict well the microphone performance. The prediction is used for better design of microphone. Previous studies (Hsu et al. 1998; Senturia 2000) presented a detailed description of this circuit, which includes radiation and compliance of the diaphragm, air-streaming resistance in the air gap and acoustic holes in back plate, and compliance of the back plate and back chamber. The mechanical components are given by the following relations:

Diaphragm radiation:

$$R_r = \frac{\rho_0 a^4 \omega^2}{2\pi c}, \; M_r = \frac{8\rho_0 a^3}{3\pi\sqrt{\pi}}. \tag{1}$$

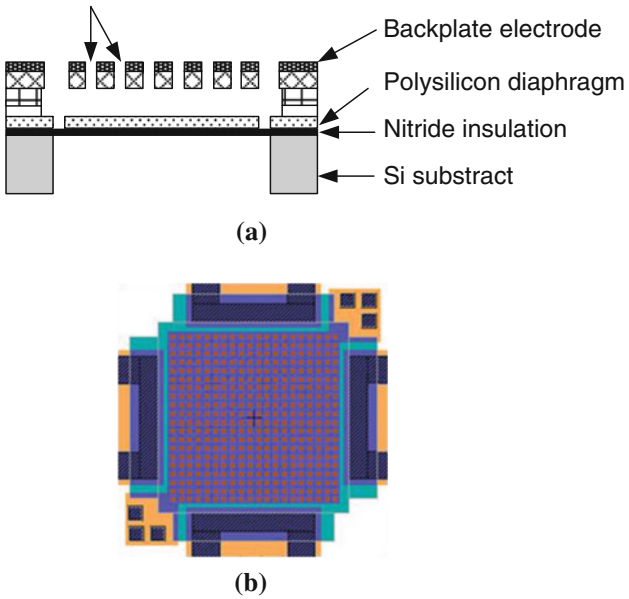

Fig. 1 **a** Structure of the MEMS microphone, **b** fabrication processes for the microphone

Diaphragm compliance and mass inertia:

$$C_m \cong \frac{32a^2}{\pi^6(2\pi^2 D + a^2 T)},\ M_m = \frac{\pi^4 \rho(2\pi^2 D + a^2 T)}{64T}. \quad (2)$$

The viscosity loss in the air gap and its compliance:

$$R_g = \frac{12ua^2}{nd^3\pi}\left(\frac{\alpha}{2} - \frac{\alpha^2}{8} - \frac{\ln\alpha}{4} - \frac{3}{8}\right),\ C_a = \frac{d}{\rho_0 c^2 \alpha^2 a^2}. \quad (3)$$

The viscosity loss of back plate holes is approximated as (Hsu et al. 1998):

$$R_h \approx \frac{8uha^2}{\pi n r^4}. \quad (4)$$

In the above equations, a is the side length of the microphone, ρ_0 is the density of air, c is the speed of sound in air, ω is the angular frequency (2πf), ρ is tensile force per unit length, n is the hole density in the backplate, α is the surface fraction occupied by the holes, u is the air viscosity coefficient, d is the average air gap distance, and h is the back plate height and r is the radius of hole. The sensitivity of the microphone is then considered as the output voltage with the presence of the acoustical pressure loading, i.e.,

$$S_e = \frac{V_0}{P} = \frac{V_b a^2}{j\omega d Z_t}, \quad (5)$$

where P is the sound pressure; V_b is the bias voltage between two electrodes; Z_t is the total equivalent impedance of the circuit; a is the width of the membrane; d is the gap distance of the microphone. The goal of our design is to maximize the sensitivity within audible frequency range, 10–10 kHz. Based on the analysis tool with Eq. (5), the microphone is designed of 1.1 μm thick and 2 × 2 mm^2. As shown herein, the baseline design determined based on the lumped coupled eletro-mechanical-acoustic model presented in this section, while the structure and geometry of the device is optimized via FEM analysis in Sect. 3, with confirmation of no pull-in occurrence in Sect. 5.

3 FEM analysis

Two commercial softwares, COMSOL and ANSYS, are utilized for predicting the capacitance of the designed microphone and the static/dynamic behaviors of the proposed MEMS microphone device, respectively. The capacitance value is first predicted by COMSOL, which is accomplished using the 3D electrostatics application mode in the electromagnetic module. The potential on each capacitor plate must obey the applied boundary condition and is therefore constant. Between the plates, the electric field is almost uniform, but fringing effects are seen at the edges of the plates. Under the proposed design dimension, the capacitance of the parallel plates, C, is calculated from the COMSOL, as shown in Fig. 2. It shows the resulted capacitance is approximately 2.4 pF by summing all the analyzed value.

Dynamic FEM analysis is next performed via ANSYS to predict pull-in and frequency response of the device. Since the mechanical force and electrostatic force are coupled, the simulation by ANSYS is carried out by a direct matrix-coupled formulation in a 3-D transducer element, TRANS126. The element couples structural motion with electrostatic fields, which can be used in a "lumped" or "distributed" environment. The capacitive microphone is seen as a pressed transducer, with the diaphragm suspended above the fixed substrate. The diaphragm is meshed with four node Solid 45 element. The top and bottom electrodes are separated by air gap, which is modeled using distributed TRANS126 transducer element (Fig. 3). All the geometry parameters must fulfill fabrication requirements, which is the major consideration of the geometrical design. The area of the diaphragm is 2 × 2 mm^2, the material properties of the diaphragm are Young's modulus E = 170 GPa, poisson's ratio v = 0.34 and the density ρ = 2,300 kg/m^2. The thickness of the diaphragm and the air gap are 1.1 and 3.75 μm, respectively. Finally, the residual stress is set as 90 MPa for FEM simulations. Simulated static deflection of the microphone membrane via ANSYS is shown in Fig. 5b, where it is seen that the microphone can be safely operated without pull-in occurring, possibly due to high membrane residual stress of 90 MPa assumed. Note that this assumed residual stress of 90 Mpa will be validated later by experiment, as stated in Sect. 5.

4 Fabrication

Figure 4a shows the cross-section of the customized hybrid processes designed and employed by this study for

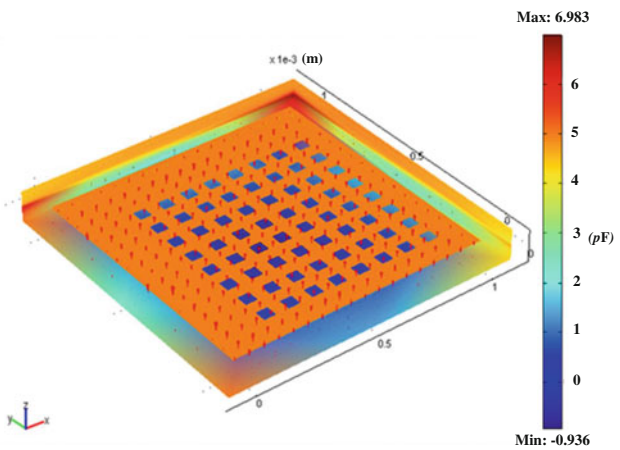

Fig. 2 Capacitance analysis by COMSOL

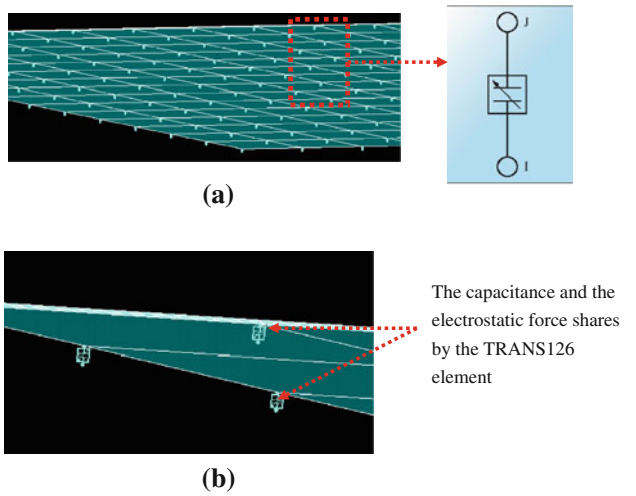

Fig. 3 **a** Schematic TRANS126 element **b** TRANS126 electro-mechanical transducer element

microphones based on the standardized processes of PolyMUMPs (Koester et al. 2003) and SOIMUMPs (Koester et al. 2003). As shown in Fig. 5, the standard PolyMUMPs process offers to deposit seven layers, consisting of four kinds of materials, on the substrate. As it creates each layer, it converges to three basic steps, including deposition, lithography and etching, to manufacture the structures, devices, or systems of micrometer size. The material layers and the lithography masks are also listed in Fig. 5. Attention has to be paid to the difference between the layer and the mask names. Using eight masks to modify different aspects of the wafer, one can create a lot of different designs on a chip. On the other hand, the process of SOIMUMPs is employed in the later steps of fabrication, which is used to do back-etching to form the membrane of microphones. The Overview of SOIMUMPs is shown in Fig. 6. In this process of fabrication, the inductively coupled plasma sputtering (ICP) technique is used to back-etch silicon substrate (the thickness is about 525 μm) to the Nitride level, the membrane of microphones is accomplished.

Employing the PolyMUMPs process, the fabrication designed for building microphone membranes in this study is started by depositing four layers, including a nitride layer called NITRIDE, three polysilicon layers (POLY0-2), two sacrificial oxide layers (OXIDE1 and OXIDE2), and a gold metal layer named METAL. Hydrofluoric (HF) acid solution is used to release the sacrificial layers of OXIDEs and to form the semi-rigid back plate fabricated by two polysilicon layers, POLY1-2. The SOIMUMPs process is finally employed for the backside bulk micromachining to form the low-stress nitride thin film (Royer et al. 1983) which is a deformed diaphragm.

In this study, three modifications are made to achieve desired microphone performance. The first one is that the

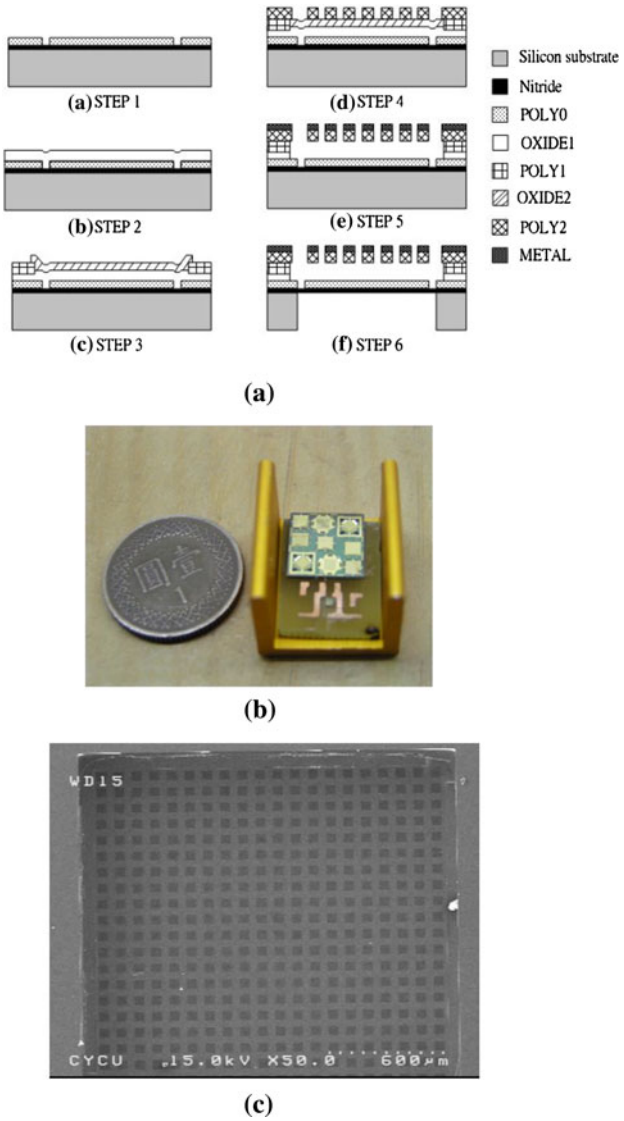

Fig. 4 **a** Fabrication processes for the microphone, **b** a photo of the fabricated microphone, **c** a micro-photo on the fabricated microphone by a scanning electron microscopic (SEM)

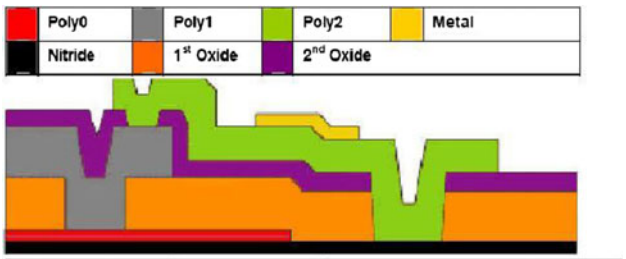

Material Layer	Thickness (μm)	Lithography Level Name
Nitride	0.6	--
Poly 0	0.5	POLY0 (HOLE0)
First Oxide	2.0	DIMPLE ANCHOR1
Poly 1	2.0	POLY1 (HOLE1)
Second Oxide	0.75	POLY1_POLY2_VIA ANCHOR2
Poly 2	1.5	POLY2 (HOLE2)
Metal	0.5	METAL (HOLEM)

Fig. 5 Overview of PolyMUMPs (Koester et al. 2003)

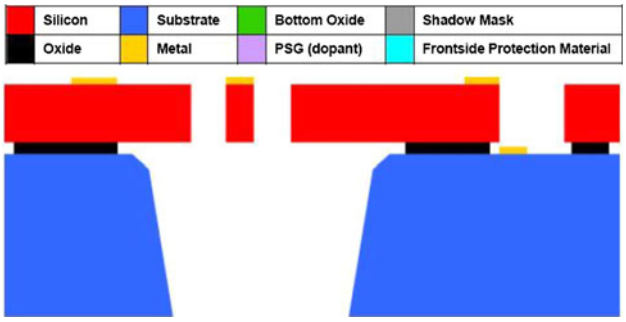

Fig. 6 Overview of SOIMUMPs (Koester et al. 2003)

thickness of layer OXIDE1 is replaced by 3 μm instead of standard 2 μm, in order to enlarge air gap, as shown in Fig. 4a. Note that this gap enlargement leads to a significantly higher sensitivity based on the design Eq. (1), and also avoid sticking during etching release. The second modification is that, unlike the standard POLY1 (Chao et al. 2006) which was doped, the layer of POLY1 is undoped to impose insulation between two charged microplates which are the diaphragm and the backplate. The last modification is that the backside etching via the standard SOIMUMPs etches the device through the substrate but stops at the nitride layer. Figure 4b shows a number of fabricated microphones in varied designed patterns, while Fig. 4c display a micro-photo on top of a given fabricated microphone membrane where holes are seen clearly in a squared membrane patterned successfully by the RIE process.

5 Experimental results

Static and dynamic experiments are conducted, respectively, to verify previous analytical predictions and predict microphone performance. In the case with a static input voltage applied to the membrane, the deflection of the entire membrane is measured by a laser Doppler vibrometer, Polytec OFV-5000. Figure 7a shows the experimental apparatus, while Fig. 7b shows the comparison results among the measurements and the simulated results using the aforementioned analytical tool in Sect. 3. With a residual stress of 90 Mpa afore-assumed, the theoretical predictions agree well with experimental counterparts, thus this 90 MPa serves legitimately as the residual stress of the membrane. It is also seen from Fig. 7b that the microphone can be safely operated without pull-in occurring up to bias of 16 V, due to high membrane residual stress of 90 MPa assumed. Since commercial microphones used in the mobile device that can only supply bias up to 5 V, the presented microphone can be safely operated in mobile phones without pull-in occurring.

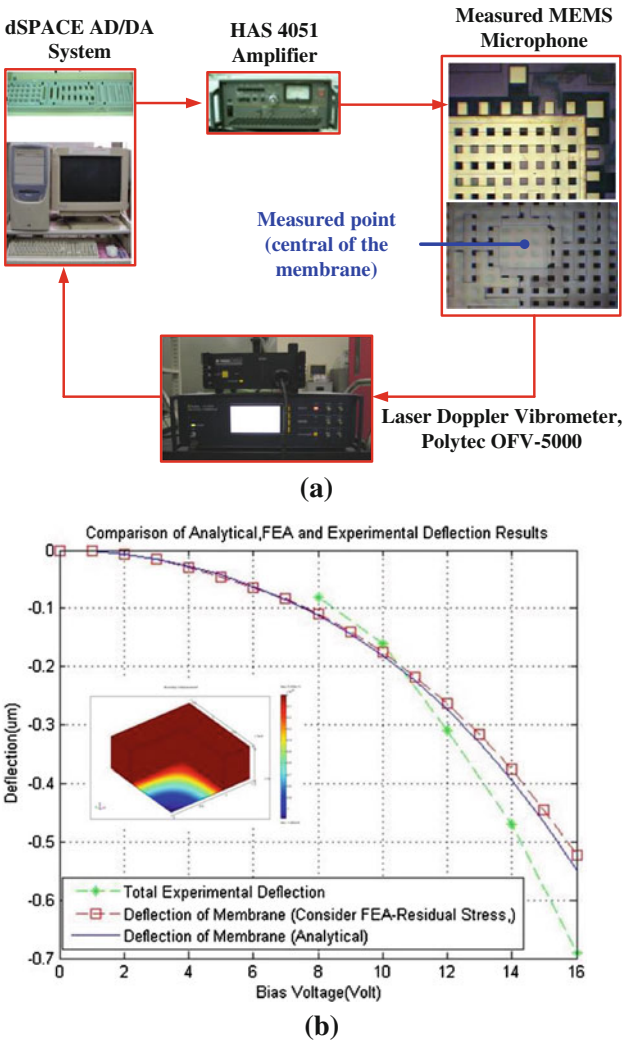

Fig. 7 **a** Experimental apparatus, **b** measured, simulated and analytical results

In order to test the sensitivity of the microphone, the device was placed in the anechoic room as shown Fig. 8. The interior of the room is covered with SONEX prospec polyurethane composite foam which provides a sound barrier to external noise and internal sound absorption. The speaker is driven with a HAS 4051 amplifier, which inputs driving signals from SRS785 dynamic signal analyzer. A reference calibrated microphone, the JEIC 1051 free-field microphone with preamplifier is used for measuring nominal ambient pressure. The measured MEMS microphone is next connected to a B&K 2671 preamplifier with an internal impedance of 1.5 GΩ. The preamplifier is connected a bias voltage supply which provides an internal DC polarization voltage for operating the designed MEMS microphone. The output voltage from the preamplifier is recorded using an SRS785 dynamical signal analyzer. Based on the recorded response from the MEMS microphone, the microphone

sensitivity is obtained by subtracting the reference response from the device response plus the calibration output level.

According to the common specifications of the commercial microphones used in the mobile device, the operation bias voltage is around 2–5 V. Therefore, two bias voltages, 2 and 4.5 V, are considered for testing the sensitivity. Figure 9 shows the measured sensitivities of the microphone. Note that since the major design criterion for microphones is to request flatness before 10 kHz to render satisfactory fidelity, thus the measurement presented herein is up to 10 kHz. It is clearly seen from this figure that with a bias voltage of 2 V, the 2 mm-sized microphone renders the sensitivity between −58 and −64 mV/Pa from 100 to 10 kHz, the audible frequency range. With bias of 4.5 V, the microphone exhibits sensitivities between −58 and −65 mV/Pa, from 100 to 10 kHz. As compared to the presented MEMS microphones, the sensitivity performance in this study, particularly 1.7 mV/Pa under bias 4.5 V, is found slightly better than those devices presented in the initial stage of MEMS microphone development (Bergqvist and Rudolf 1990; Scheeper et al. 1992, 1994) [around 1 mV/Pa with bias 2 V and above, as shown in (Scheeper et al. 1992)], while compatible to some most recent developed devices (Lee et al. 2012; Ganjia and Majlis 2009). The devices developed by the current study is however inferior to those recently developed in academia (Pedersen et al. 1998; Hsu et al. 1998) and industry (Knowles Company 2013), by which the sensitivity could reach 10 mV/Pa, with an integrated CMOS pre-amplifier and/or low residual stress in microphone membrane. Note that the current study aims mainly to showcase the feasibility of a hybrid process combining two available stable PolyMUMP and SOIMUMP to increase yield rate. The sensitivities and signal-to-noise ratio (SNR) can be further increased in the future by a better readout circuitry and techniques of signal processing.

As to the bandwidth of the microphone, also shown in Fig. 9, the presented microphone offers relatively linear response up to 10 kHz, the performance of which is compatible to other already existing ones. In fact, under the measured audible range, the proposed device with bias 4.5 V maintains the loss as less as 2.7 dB (ref. to V/Pa), under 3 dB—the commonly acceptable drop before the upper limit of the audible frequency range, 10 kHz (Pedersen et al. 1998). However, small levels of fluctuation in both responses in Fig. 9 along the increasing frequency are present, which could cause distortion in output sound signal. This is due to the low fabrication quality by

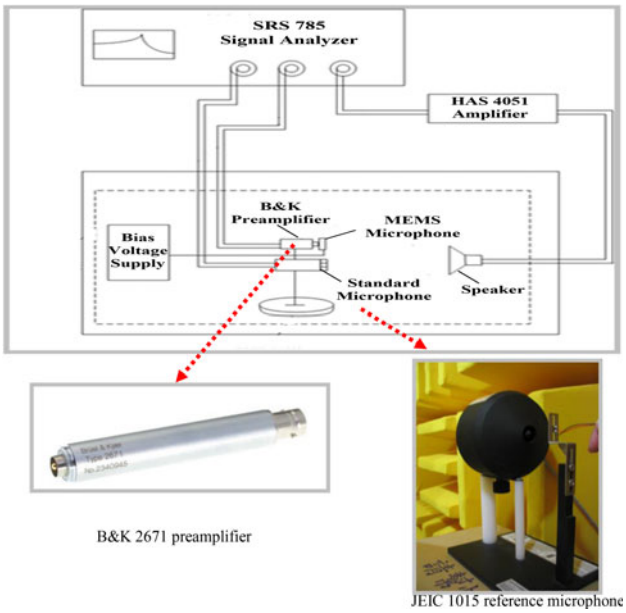

Fig. 8 Experimental apparatus in anechoic room

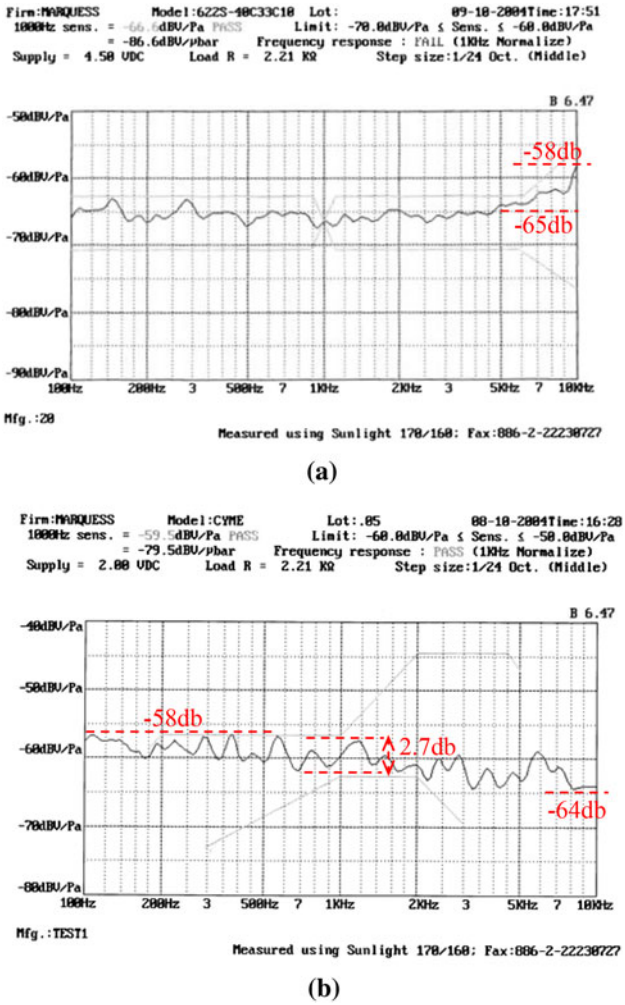

Fig. 9 Frequency response of a 2.0 mm wide microphone **a** with a bias voltage of 4.5 V, the microphone exhibits sensitivity between −65 and −58 dB from 100 to 10 kHz, **b** with a bias voltage of 2 V, the 2 mm-wide microphone has a sensitivity between −58 and −64 dB

preliminary fabrication trails, which leads to nonlinear, asymmetric and non-uniform distributions of mechanical/electrical properties over the membrane, such as membrane thickness and residual stress. It is possible to improve fabrication quality along the development of mass production. Note lastly on frequency response that the phase response is not presented and discussed herein. This is due to the fact that the major cause of phase delay for a microphone unit comes from electronic readout circuit, not the device membrane (Chiang et al. 2012), since only the factor of material damping of the membrane in the device leads to phase delay, which is usually much less than that caused by readout circuitry.

6 Conclusion and future works

A single-chip-processed silicon condenser microphone has been designed and fabricated. The microphone with a thin membrane of 2×2 mm^2 in area and a thick backplate are fabricated. The analysis via finite-element (FEM) and equivalent circuit are successfully conducted to design and evaluate the microphone. The integration of standard PolyMUMPs and SOIMUMPs processes is proposed, where the sacrificial layer sizes are re-assigned to successfully develop a microphone structure with better sensitivity. Static membrane deflection are also simulated and measured by computer software and a laser Doppler vibrometer, respectively. It is confirmed that no pull-in occurs for normal microphone operations.

The sensitivity of the fabricated microphone within audible range is measured. The measured sensitivity of the microphone is around 0.78 and 1.7 mV/Pa from 100 to 10 kHz, under the biases of 2 and 4.5 V, respectively. This sensitivity performance is compatible to some microphones presented in the past. The device also maintains the loss as less as 2.7 dB (ref. to V/Pa), under 3 dB—the commonly acceptable drop within the audible frequency range. To increase the sensitivity in the future, the residual stress of the membrane ought to be reduced by lowering deposition temperature of membrane material. Further efforts are to improve fabrication quality, for lessening negative effects of nonlinear, asymmetric and non-uniform distributions of mechanical/electrical properties over the membrane, and also to perform drop tests (Meng et al. 2012) for fortify the device structure against accidental drops.

Acknowledgments The authors appreciate the support from National Science Council of R.O.C under the grant no. NSC 101-2623-E-009-006-D and 100-2221-E-009-091-. This work was also supported in part by the UST-UCSD International Center of Excellence in Advanced Bio-Engineering sponsored by the Taiwan National Science Council I-RiCE Program under Grant NSC-100-2911-I-009-101.

References

Bergqvist J (1993) Finite-element modeling and characterization of a silicon condenser microphone with a highly perforated backplate. Sens Actuators 39:191–200

Bergqvist J, Rudolf F (1990) A new condenser microphone in silicon. Sens Actuators 21:123–125

Chan C-K, Lai W-C, Wu M, Wang M-Y, Fang W (2011) Design and implementation of a capacitive-type microphone with rigid diaphragm and flexible spring using the two poly silicon micromachining processes. IEEE Sens J 11:2365–2371

Chao PC-P, Chiu C-W, Tsai C-Y (2006) A novel method to predict the pull-in voltage in a closed form for micro-plate actuated by a distributed electrostatic force. J Micromech Microeng 16:986–998

Chao PC-P, Chiu C-W, Liu T-H (2008) DC dynamic pull-in predictions for a generalized clamped–clamped micro-beam based on a continuous model and bifurcation analysis. J Micromech Microeng 18:14

Chen J-M, Kuo C-F, Wang D-B, Huang C-W, Sun S-C, Hsieh Y-S, Zhon W-Z (2010) Low bias voltage and high sensitivity CMOS condenser microphone using combined stress relaxation design. The 5th International Conference on Microsystems Packaging Assembly and Circuits Technology, pp 1–3

Chiang C-T, Wang C-H, Wu C-Y (2012) A CMOS MEMS audio transducer implemented by silicon condenser microphone with analog front-end circuits of audio codec. IEEE Trans VLSI Syst J 20(9):1656–1667

Ganjia BA, Majlis BY (2009) Design and fabrication of a new MEMS capacitive microphone using a perforated aluminum diaphragm. Sens Actuat A 149:29–37

Hsu PC, Mastrangelo CH, Wise KD (1998) A High sensitivity polysilicon diaphragm condenser microphone. In: The 11th Annual International Conference on MEMS, Heidelberg, pp 580–585

Knowles Company (2013) Datasheet of the SP-series MEMS Microphone, http://www.knowles.com/search/products/m_surface_mount.jsp

Koester ID, Cowen A, Mahadevan R, Stonefield M, Hardy B (2003) PolyMUMPs^{TM} Design Handbook. Revision 10.0, MEMSCAP

Koester ID, Cowen A, Mahadevan R, Stonefield M, Hardy B (2003) SOIMUMPs^{TM} Design Handbook. Revision 3.0, MEMSCAP

Lee J, Je CH, Yang WS, Kim Y-G, Cho M-H, Kim J (2012) Thin MEMS microphone based on package-integrated fabrication process. Electron Lett 48(14):29–37

Leinenbach C, van Teeffelen K, Laermer F, Seidel H (2010) A new capacitive type MEMS microphone. The IEEE 23rd International Conference on MEMS, pp 659–662

Meng J, Mattila T, Dasgupta A, Sillanpaa M, Jaakkola R, Andersson K, Hussa E (2012) Testing and multi-scale modeling of drop and impact loading of complex MEMS microphone assemblies. The 13th International Conference on Thermal, Mechanical and Multi-Physics Simulation and Experiments in Microelectronics and Microsystems (EuroSimE) vol 14. pp 1/8–8/8

Pedersen M, Olthuis W, Beergvld P (1998) High performance condenser microphone with fully integrated CMOS amplifier and DC–DC voltage converter. JMEMS 7:387–394

Royer M, Holmen JO, Wurm MA, Aadland OS, Glenn M (1983) ZnO on Si integrated acoustic sensor. Sens Actuators 4:357–362

Scheeper PR, van der Donk AGH, Olthuis W, Bergveld P (1992) Fabrication of silicon condenser microphones using single wafer technology. JMEMS 1:147–154

Scheeper PR, van der Donk AGH, Olthuis W, Bergveld P (1994) A review of silicon microphones. Sens Actuators 44:1–11

Senturia SD (2000) Microsystems Design. Kluwer Academic Publishers, pp 397–428

Wang WJ, Lin RM, Zou QB (2004) Modeling and characterization of a silicon condenser microphone. JMEMS 14:403–409